ACS Catalysis

Research Article

pubs.acs.org/acscatalysis

Water-Promoted O_2 Dissociation on Small-Sized Anionic Gold Clusters

Yi Gao*,† and Xiao Cheng Zeng*,‡

†Laboratory of Physical Biology and Division of Interfacial Water, Shanghai Institute of Applied Physics, Chinese Academy of Sciences, Shanghai 201800, China

‡Department of Chemistry, University of Nebraska−Lincoln, Lincoln, Nebraska 68588, United States

Supporting Information

ABSTRACT: Although thermodynamically O_2 favors dissociative adsorption over molecular adsorption on small-sized anionic gold clusters (except Au_2^-), O_2 dissociation is unlikely to proceed under ambient conditions because of the high activation energy barrier (>2.0 eV). Here, we present a systematic theoretical study of reaction pathways for the O_2 dissociation on small-sized anionic gold nanoclusters Au_n^- (n = 1−6) with and without involvement of a water molecule. The density functional theory calculations indicate that the activation barriers from the molecular adsorption state of O_2 to dissociative adsorption can be significantly lowered with the involvement of a H_2O molecule. Once the O_2 dissociates on small-size gold clusters, atomic oxygen is readily available for other reactions, such as the CO oxidation, on the surface of gold clusters. This theoretical study supports previous experimental evidence that H_2O can be used to activate O_2, which suggests an alternative way to exploit catalytic capability of gold clusters for oxidation applications.

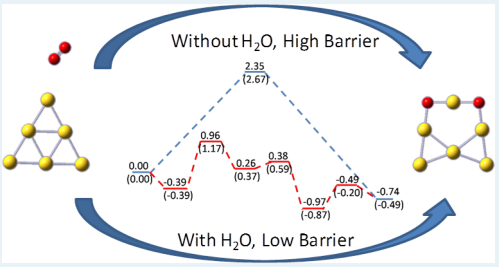

KEYWORDS: *O_2 dissociation, small-sized anionic Au clusters, water promotion, nanocatalysts*

INTRODUCTION

Small-sized gold clusters have attracted wide attentions because of their extraordinary catalytic activities in chemical reactions.[1−20] In 1987, Haruta et al. discovered that gold nanoparticles can be active catalysts for CO oxidation much below room temperature.[1] Thereafter, a vast class of oxygen-atom transfer reactions has been shown to be enhanced by nanogold catalysts under ambient conditions of temperature and humidity.[2−5] These reactions include the full or partial combustion of noxious gas, water-gas shift, and styrene epoxidation, among others;[12−20] however, detailed reaction mechanisms for the oxidation are still not completely understood because of the lack of structural information of O_2 on gold nanoclusters.

Early investigation by Cox et al. showed that even-sized Au_n^- clusters up to n = 20 give rise to measurable adsorption of O_2 based on helium flow-reactor method.[21,22] Ervin and co-workers investigated reaction kinetics on the three smallest even-sized gold anion clusters (Au_2^-, Au_4^- and Au_6^-) with O_2 and estimated the adsorption energy by collision-induced dissociation methods.[23] Whetten and co-workers studied O_2 adsorption on Au_n^- clusters for n = 2−22. Their experiments demonstrated that odd-sized gold anion clusters are inert to the O_2 adsorption and that even-sized gold anion clusters can adsorb a single O_2 molecule.[24,25] Wang and co-workers performed a joint experimental photoelectron spectroscopy (PES) and density functional theory (DFT) calculation study of O_2 adsorptions on the smallest even-sized anionic Au_n^- clusters. They demonstrated molecularly chemisorption of O_2 on Au_n^- (n = 2, 4, 6) and physisorption of O_2 on Au_n^- (n = 1, 3, 5).[26] A recent joint experimental PES and theoretical study shows that a superoxo (nonbridging) to peroxo (bridging) transition for the O_2 chemisorption on anionic gold clusters occurs at Au_8^-.[27] This observation is also reported by Woodham et al. on the basis of a joint vibrational spectroscopy/DFT study.[28]

Numerous theoretical studies have also been devoted to the explanation of previous experimental observations. Mills, Gordon, and Metiu examined O_2 binding on small-sized Au_n and Au_n^- clusters and found O_2 binds more strongly to clusters with an odd number of electrons than with an even number.[29] Ding et al. tested a hybrid DFT method to compare with experimental results and found their calculation results are consistent with measured adsorption of O_2 on anionic, cationic and neutral Au_n (n = 1−6).[30] Molina and Hammer studied O_2 adsorption on Au_n (n = 1−11) with and without a support.[31] Barton and Podkolzin employed a model system to show sensitivity of O_2 adsorption to the clusters' size.[32] Yoon et al. studied both molecular and dissociative adsorption of O_2 on anionic gold clusters Au_n^- (n < 8).[33] They suggested that molecular adsorption is more favorable for $n \leq 3$, whereas dissociative adsorption is energetically more favorable for larger clusters. They also showed that the dissociation would encounter a very high barrier. Wang and Gong investigated

Received: June 14, 2012
Revised: September 10, 2012
Published: October 23, 2012

   dx.doi.org/10.1021/cs300383p | ACS Catal. 2012, 2, 2614−2621

O_2 chemisorption on Au_{32}, and they found the oxygen dissociation is more favorable than molecular adsorption.[34] Barrio et al. used Au_{14}, Au_{25}, and Au_{29} as model systems to demonstrate the importance of cluster geometry to the O_2 adsorption energies.[35] Lyalin and Takersugu investigated the relative stability between molecular and dissociative adsorption of O_2 on odd-size Au_n (n = 1, 3, 5, 7, 9) using a DFT method. They found that molecular adsorption of O_2 is more favorable for two-dimensional (2D) Au_n (n = 1, 3, 5, 7), whereas dissociative adsorption is more favorable for 3D Au_n clusters (n = 9).[36]

Although dissociative adsorption of O_2 is energetically more favorable than the molecular adsorption, little experimental evidence of dissociative adsorption of O_2 has been reported, largely because of the high dissociation barrier.[33,37,38] Nevertheless, several recent experiments on gold-cluster-catalyzed CO oxidation indicate that the presence of water molecules may promote O_2 dissociation, which will facilitate the CO oxidation.[39] Boccuzzi and Chiorino suggested that the dissociation of O_2 might be needed to observe the oxidation reaction. Haruta et al. proposed possible reaction steps involving water molecules, on the basis of their experimental observation of the moisture effect on CO oxidation.[40,41] Bongiorno and Landman showed theoretical evidence of enhancement of the catalytic activity with the presence of water on either free or supported gold clusters.[42] The experiments by Mullins and co-workers demonstrated the direct involvement of water in CO oxidation, where the OH is a possible reaction intermediate.[43] Wallace et al. studied oxygen adsorption on hydrated gold cluster anions.[44] Their results indicated that the binding of an OH group will enhance the reactivity toward molecular oxygen on odd-sized anionic gold clusters, but lower the reactivity on even-sized ones. Okumura et al. performed DFT calculations to examine the coadsorption of H_2O and O_2 on neutral and anionic Au_{10} clusters. They found that the negatively charged Au_{10}^- cluster can greatly increase the coadsorption.[45] Zhang et al. explored theoretically the pathway for the CO oxidation on the Au(111) surface in the presence of water.[46] Lee et al. performed a combined experimental and theoretical study to show that the water vapor can facilitate the selectivity of propane epoxidation on immobilized Au_{6-10} clusters.[47]

Although extensive work has been done regarding O_2 adsorption on Au clusters and related dissociation of O_2 in the presence of water, a systematic study of water-promoted O_2 dissociation on gold clusters is still lacking. In this article, we present a comprehensive theoretical study of O_2 dissociation on small-sized anionic gold clusters (Au_n^-, n = 1–6). We show calculation results that the high O_2 dissociation barrier can be greatly lowered with the presence of a water molecule nearby. Therefore, this study provides additional insights into oxidation mechanism with gold nanocatalysts.

COMPUTATION METHODS

All calculations are based on methods of DFT. Specifically, two hybrid functionals (i.e. the Becke's three parameter hybrid functional with the Lee–Yang–Parr correlation (B3LYP) functional[48,49]) and the Tao–Perdew–Staroverov–Scuseria (TPSSh) functional are employed.[50] The B3LYP functional can provide reliable O_2 adsorption energies consistent with the experiments,[30] and the TPSSh functional has been proven to be one of the best functionals to evaluate relative stabilities among isomers of gold cluster.[51] The Stuttgart/Dresden effective core potential valence basis[52,53] augmented with two sets of f functions (exponents = 1.425, 0.468) and one set of g function (exponent = 1.147) is adopted for Au, and the 6-311+G(d,p) basis sets are used for O and H. The basis-set superposition error (BSSE) is corrected using the counterpoise method. The doublet spin state is considered as the most favorable for even-sized anionic Au clusters binding with O_2, whereas both the singlet and triplet spin states are considered for the odd-sized anionic Au clusters binding with O_2. All energies in the reaction pathways and corresponding geometries for the singlet and triplet states of odd-sized anionic gold clusters are given in the Supporting Information (Figure S2–S4). The transition-state structures are searched by using the synchronous transit-guided quasi-Newton method developed by Schlegel and co-workers.[54,55] All cluster structures are fully optimized, and their local stabilities are confirmed from vibrational frequency calculation. The transition states entail only one imaginary vibrational frequency. The zero-point energies are included in the reaction pathway. All the calculations are carried out using the Gaussian 09 software package.[56]

RESULTS AND DISCUSSIONS

Molecular Adsorption of O_2. Optimized geometries of $Au_nO_2^-$ (n = 1–6) are plotted in Figure 1, where O_2 is in molecular form upon binding with the gold clusters. All the anionic Au clusters adopt the 2D structures because of their higher stabilities with respect to the 3D structures, as discussed elsewhere.[8,57] It is worth noting that there are several competing isomers for Au_4^-–Au_6^- (see Figure S1), and the structures adopted here were considered as model structures, as in previous studies of the O_2 adsorption (see Table 1) and catalysis.[25,30,58] In Table 1, the adsorption energies calculated on the basis of TPSSh and B3LYP functionals are listed to compare with previous theoretical and experimental results. One can see that (1) TPSSh calculations predict greater adsorption energies and shorter bond lengths than B3LYP calculations. (2) The results from B3LYP calculations are consistent with those by Ding et al.,[30] although much larger

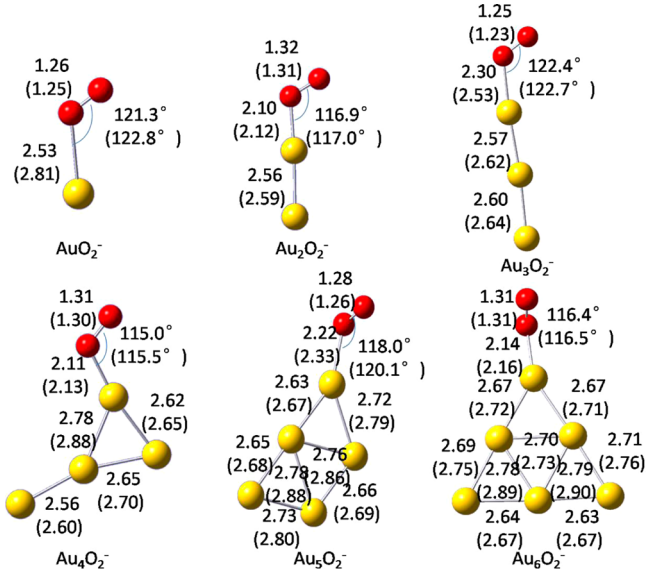

Figure 1. Optimized lowest-energy geometries of $Au_nO_2^-$ (n = 1–6) based on the TPSSh (B3LYP in parentheses) level of theory. All the lengths marked are in angstroms.

dx.doi.org/10.1021/cs300383p | ACS Catal. 2012, 2, 2614–2621

Table 1. Calculated Binding Energies (eV) of Molecular O_2 on Au_n^- Anionic Clusters (n = 1-6)

	this work							
	TPSSh[a]	B3LYP[a]	TPSSh[b]	B3LYP[b]	B3LYP[c]	PW91[c]	PW91	exp[f]
AuO_2^-	−0.37	−0.30	−0.41	−0.31	−0.22	−0.44	−0.50[d]	
$Au_2O_2^-$	−1.25	**−1.07**	−1.56	−1.41	−0.95	−1.24	−1.40[d]	**−1.01 ± 0.14**
$Au_3O_2^-$	−0.22	−0.09	−0.22	−0.07	−0.04	−0.33	−0.37[d]	
$Au_4O_2^-$	−1.03	**−0.82**	−1.27	−1.12	−0.72	−1.03	−1.19[d]	**−0.91 ± 0.14**
$Au_5O_2^-$	−0.38	−0.17	−0.48	−0.23	−0.07	−0.44	−0.61[e]	
$Au_6O_2^-$	−1.05	**−0.89**	−1.35	−1.24	−0.78	−1.01	−1.06[e]	**∼−0.81**

[a]SDD+2f1g for Au, 6-311+G(d) for O; without BSSE corrections. [b]SDD+2f1g for Au, 6-311+G(d) for O; with BSSE corrections. [c]Ref 30, LANL2DZ for Au, 6-311+G(3df) for O. [d]Ref 27, plane-wave basis. [e]Ref 33, plane-wave basis. [f]Ref 26. Experimental values are given here.

basis sets are used here. This means that the interaction between O_2 and anionic Au clusters are not very sensitive to the basis sets selected. (3) O_2 can be strongly adsorbed on even-sized Au anionic clusters, but very weakly adsorbed on odd-sized Au anion clusters, consistent with previous experimental measurements.[21,22,25] (4) O_2 is located within the same plane as planar Au_n^- (n = 2−4) clusters, but located out of the plane of the planar Au_5^- and Au_6^- clusters, consistent with Yoon's results.[33] (5) The O−O bond length in even-sized anionic Au clusters ($Au_2O_2^-$, 1.32 Å; $Au_4O_2^-$, 1.31 Å; $Au_6O_2^-$, 1.31 Å) is longer than that in odd-sized Au clusters (AuO_2^-, 1.26 Å; $Au_3O_2^-$, 1.25 Å; $Au_5O_2^-$, 1.28 Å). (6) The binding energies with BSSE corrections are greater than those without corrections, especially for the even-sized anionic Au clusters. This is due to obvious electron transfer from anionic Au clusters to O_2 (see below). As a result, the ground state of O_2 is no longer in the triplet state. In addition, we computed the binding energies with larger basis sets (Supporting Information Table S1) and found the results show little change.

The charge transfer from the Au cluster to O_2 molecule has been considered as a major factor that correlates with the adsorption strength. The Mulliken charge analysis gives rise to a notable odd−even oscillation for the electron transfer; that is, the even-sized Au anionic clusters transfer more electrons to the O_2 molecule ($Au_2O_2^-$, 0.47e; $Au_4O_2^-$, 0.40e; $Au_6O_2^-$, 0.39e) than odd-sized Au anionic clusters (AuO_2^-, 028e; $Au_3O_2^-$, 0.11e; $Au_5O_2^-$, 0.24e). This result is consistent with a previous one based on natural population analysis (NPA).[59] Note also that more electron transfer can lead to a longer Au−O bond length, which explains the odd−even oscillation of the Au−O bond-length.

O_2 Splitting on Au_n^- Anionic Clusters. *AuO_2^-*. Dioxygen adsorption on Au^- anion has been discussed in a recent joint experimental PES and ab initio study,[37,38] but the reaction pathway has not been reported in the literature. In Figure 2, we present a reaction pathway of O_2 splitting, with and without involvement of a water molecule. In the DFT calculation, both TPSSh and B3LYP calculation results indicate that the AuO_2^- dioxide isomer and O_2 physisorbed isomer $Au^-(O_2)$ are in triplet states, and the former is lower in energy than the latter (TPSSh, −0.85 eV; B3LYP, −0.48 eV), consistent with coupled-cluster CCSD(T) calculation.[37,38] In addition, we compute the transition state connecting the two isomers. A very high activation barrier (TPSSh, 2.96 eV; B3LYP, 3.11 eV) is found, indicating the O_2 splitting cannot occur at ambient temperature. This conclusion is consistent with recent experimental results in that the AuO_2^- dioxide isomer can be produced only under high-temperature conditions, whereas the physisorbed $Au^-(O_2)$ complex can be observed at low temperature. It should be noted that the transition state (TS)

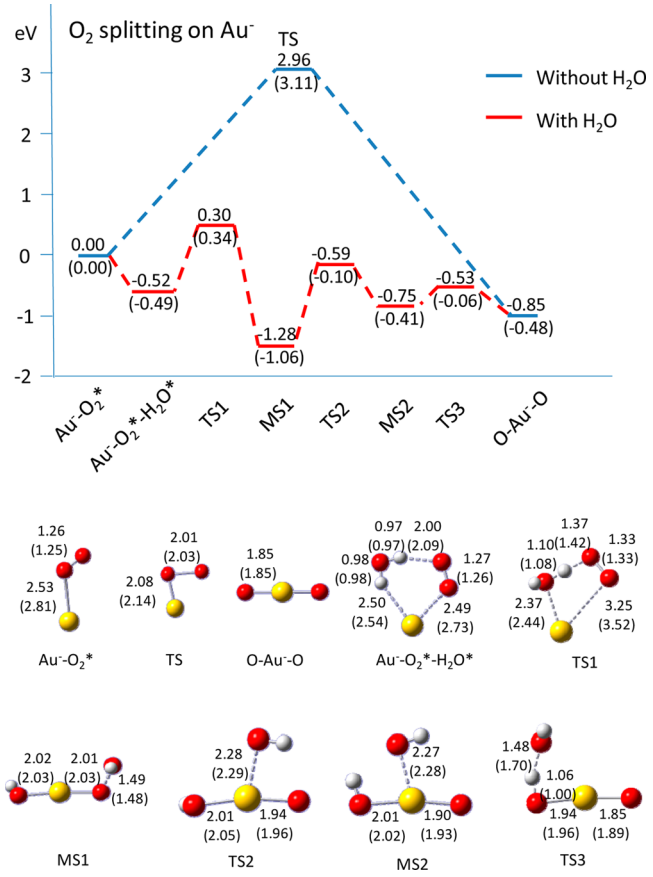

Figure 2. Calculated reaction pathway from the $Au^-(O_2)$ complex to dissociative O−Au^-−O dioxide species using the TPSSh level of theory (B3LYP results in parentheses). The unit of bond length is the angstrom; an asterisk indicates the binding state.

is a triplet state, and the singlet state is slightly higher in energy (0.11 eV higher in TPSSh calculation).

Furthermore, we show that when a water molecule is involved in the O_2 splitting, the activation barriers are significantly lowered. Previous experiments have shown that an extended and clean gold surface appears to be hydrophilic.[60] Theoretical calculations also indicate water can be adsorbed on a free or on a supported Au cluster with adsorption energy ranging from 0.2 to 0.6 eV.[37,38] Our recent CCSD(T) calculations showed that H_2O and Au^- can form a stable complex with a binding energy of 0.55 eV.[38] Here, the TPSSh calculations give a binding energy of 0.60 eV between H_2O and Au^-, close to the CCSD(T) result. If Au^- already adsorbs an O_2 molecule to form an $Au^-(O_2)$ complex, the binding energy between H_2O and the $Au^-(O_2)$ complex is 0.52 eV (TPSSh

calculation), smaller than the binding energy between H_2O and Au^-. Thus, little cooperativity is observed for the coadsorption of O_2 and H_2O on Au^- on basis of our DFT calculations.

In the second step for the O_2 splitting, O_2 captures one H atom from H_2O, for which the activation barrier is 0.82 eV (TPSSh), and the intermediate species include an OH group and a hydroperoxyl-like (HO_2) group (MS1), as predicted by Landman and co-workers.[42] In the third step, the HO_2 group can further split into an OH group and O atom, arriving at the second intermediate state (MS2). The activation barrier of this step is 0.69 eV (TPSSh). After the formation of two OH groups, one H atom can easily migrate from one group to another to form a H_2O molecule and an AuO_2^- dioxide species via crossing an activation barrier of 0.22 eV (TPSSh). A comparison of the reaction pathway for O_2 splitting with and without water clearly demonstrates that the water molecule can significantly lower the activation barrier and promote the reaction. The total activation energy for O_2-splitting with water is relatively low (TPSSh, 0.30 eV; B3LYP, 0.34 eV), implying that O_2 splitting could proceed at ambient conditions with the involvement of H_2O. Note that the first intermediate state, MS1 (HO_2), is actually lower in energy than the dioxide state (Figure 2) and the activation barrier from MS1 to MS2 ($HO_2 \rightarrow O + OH$) is 0.69 eV. If the reductant (CO or pyrene) was introduced into the system, there would be competing reactions between reductant and HO_2, which might explain the production of ·OH/·OOH which was believed to promote the partial oxidation on gold.[47,61]

$Au_2O_2^-$. As shown in Scheme 1, the linear dioxide isomer **2c**[51] is 0.83 eV higher in energy (TPSSh calculation) than the

Scheme 1. Binding Energy of Three Low-Energy $Au_2O_2^-$ Isomers

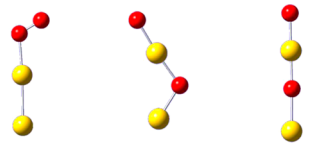

	2a	2b	2c
TPSSh	-1.25 eV	-0.85 eV	-0.42 eV
B3LYP	-1.07 eV	-0.48 eV	0.01 eV
Spin	1/2	1/2	3/2

molecular O_2 binding structure **2a** and also 0.43 eV higher than another $Au_2O_2^-$ dioxide isomer **2b**. In Figure 3, we present a reaction pathway for the O_2 splitting on Au_2^- anionic cluster. Since the dioxide species of $Au_2O_2^-$ is less stable than the $Au_2^-(O_2)$ complex, $Au_2O_2^-$ favors the molecular binding state. Moreover, the high activation barrier (TPSSh, 2.58 eV; B3LYP, 2.56 eV) would prevent O_2 from splitting directly on the Au_2^- anion at ambient conditions. When an H_2O molecule is introduced into the system, a $Au_2^-(O_2)$ complex could cross a relatively low activation barrier (TPSSh, 1.39 eV; B3LYP, 1.72 eV) to form $Au_2O_2^-$ dioxide at higher temperatures. However, there are some differences in the reaction pathway for the O_2 splitting on Au_2^- and on Au^-: (1) There is a slight energy enhancement (−0.02 eV) in the coadsorption of O_2 and H_2O on Au_2^-, whereas there is none for Au^-. (2) The $Au_2^-{-}O_2{-}H_2O$ complex is more stable than the MS1 state (with HO_2), as opposed to the less stable than MS1 state on Au^-. (3) Although the activation barrier for $Au_2^-(O_2)$ is 1.39 eV, much higher

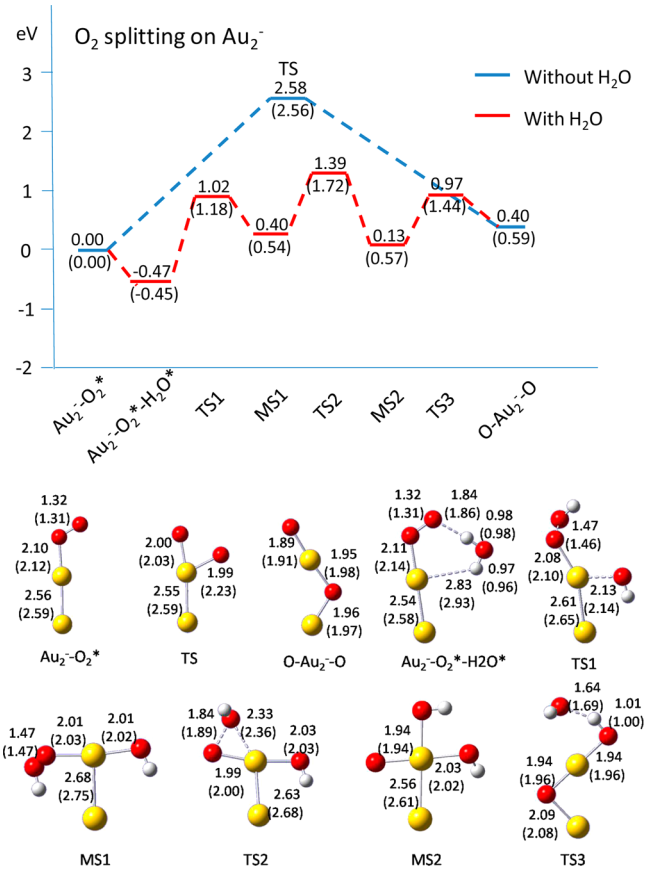

Figure 3. Calculated reaction pathway from the $Au_2^-(O_2)$ complex to dissociative $O{-}Au_2^-{-}O$ using the TPSSh level of theory (B3LYP results in parentheses). The unit of bond length is the angstrom; an asterisk means on the binding state.

than that for $Au^-(O_2)$ (0.30 eV), the relatively high preadsorption energy of O_2 on Au_2^- might lower the dissociation barrier for the entire reaction.

$Au_3O_2^-$. The reaction pathway of O_2 splitting on Au_3^- is very similar to that on Au_2^- and Au^-, as shown in Figure 4. In Scheme 2, the $Au_3O_2^-$ dioxide isomer **3b** is more stable by 0.85 eV (TPSSh calculation) than the dissociative isomer **3c**.[51] Thus, **3b** is used as the final state in the calculation of the reaction pathway. Furthermore, **3b** is lower in energy than the $Au_3^-(O_2)$ complex **3a**, which means the dioxide species is thermodynamically more stable. The binding of H_2O on $Au_3O_2^-$ (TPSSh, −0.29 eV, B3LYP, −0.26 eV) is weaker than that on $Au_2O_2^-$ (TPSSh, −0.47 eV, TPSSh, −0.45 eV) and AuO_2^- (TPSSh, −0.52 eV, B3LYP, −0.49 eV), but the participation of H_2O in the reaction can also significantly lower the activation barrier for the O_2 splitting on Au_3^-. Indeed, the activation barrier is reduced from 2.65 eV with no water to 0.79 eV with water (TPSSh calculation). The actual dissociation barrier might be even lower because of some contribution from the favorable O_2 binding. In addition, the HO_2 intermediate (MS1) is the most stable along the reaction path, similar to the case with Au^- anion.

$Au_4O_2^-$. The reaction pathway for the O_2 splitting from the $Au_4^-(O_2)$ complex to dissociative $O{-}Au_4^-{-}O$ is shown in Figure 5. The activation barrier is 2.57 eV without H_2O and 1.05 eV with H_2O on the basis of the TPSSh calculation. Although the reaction pathway is very similar to that for $Au^-{-}Au_3^-$ anions, there exists an obvious difference. The reaction

dx.doi.org/10.1021/cs300383p | ACS Catal. 2012, 2, 2614−2621

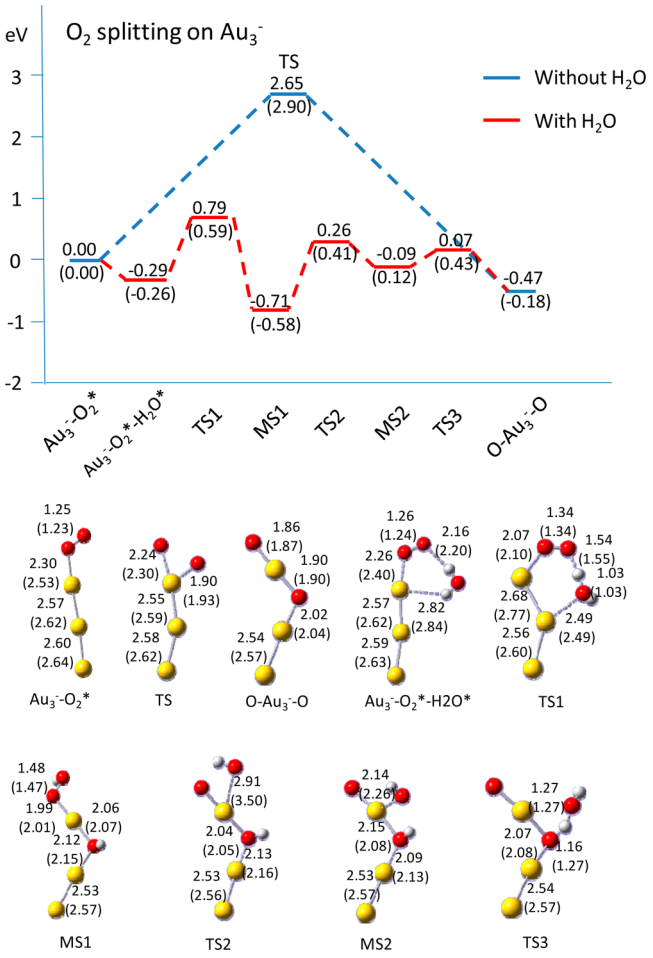

Figure 4. Calculated reaction pathway from the $Au_3^-(O_2)$ complex to dissociative $O{-}Au_3^-{-}O$ using the TPSSh level of theory (B3LYP results in parentheses). The unit of bond length is the angstrom; an asterisk means on the binding state.

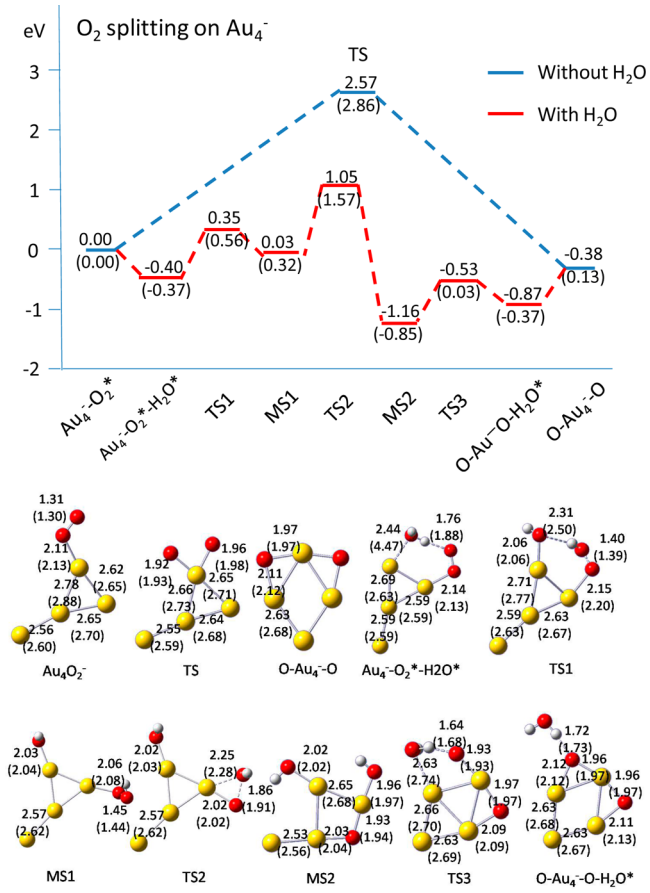

Figure 5. Calculated reaction pathway from the $Au_4^-(O_2)$ complex to dissociative $O{-}Au_4^-{-}O$ using the TPSSh level of theory (B3LYP results in parentheses). The unit of bond length is the angstrom; an asterisk indicates the binding state.

Scheme 2. Binding Energy of Three Low-Energy $Au_3O_2^-$ Isomers

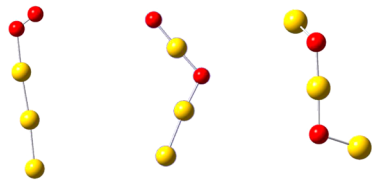

	3a	3b	3c
TPSSh	-0.22 eV	-0.69 eV	0.16 eV
B3LYP	-0.09 eV	-0.27 eV	0.52 eV
Spin	1	1	0

step from the HO_2 state (MS1 in Figure 5) to the dihydroxyl group state (MS2 in Figure 5) is exothermic for Au_4^- but endothermic for $Au^-{-}Au_3^-$. The difference in energy change is likely due to a distinct geometric change of Au_4^- (fluxional) during the reaction process, that is, the transformation of the dihydroxyl group state to the most stable state (MS2) in the reaction pathway for Au_4^-. In addition, comparing to the final dioxide states $O{-}Au_n^-{-}O$, the most stable intermediate state (MS2, the dihydroxyl group state for Au_4^-) entails the largest energy difference for Au_4^- (TPSSh: −0.78 eV), as opposed to smaller energy differences for Au^- to Au_3^- (TPSSh: −0.43 eV (Au^-), −0.27 eV (Au_2^-), −0.24 eV (Au_3^-)).

$Au_5O_2^-$. Figure 6 displays the reaction pathway for the O_2 splitting from $Au_5^-(O_2)$ complex to dissociative $O{-}Au_5^-{-}O$. The dioxide isomer $O{-}Au_5^-{-}O$ is −0.54 eV (TPSSh result) with respect to the O_2 physisorbed isomer $Au_5^-(O_2)$. The activation barrier is 0.12 eV (TPSSh calculation) with H_2O, greatly lower than that without H_2O (TPSSh: 1.81 eV). The significant distinction of this reaction pathway is the extraordinary stability of the dihydroxyl state (MS2), which is 2.36 eV lower in energy than the $Au_5^-(O_2)$ complex. This stable intermediate indicates it is very likely to carry out partial oxidation channel if the reductant is introduced into the system.

$Au_6O_2^-$. The global minimum of Au_6^- is a planar triangle structure.[57] Our TPSSh calculation suggests that the dissociative state $O{-}Au_6^-{-}O$ is 0.74 eV lower in energy than the molecular adsorption state $Au_6^-(O_2)$, consistent with previous calculations.[33] In Figure 7, we present the reaction pathway for the O_2 splitting from the $Au_6^-(O_2)$ complex to the dissociative $O{-}Au_6^-{-}O$. The activation barrier is 2.35 eV (TPSSh calculation), consistent with a previous calculation.[33] With the involvement of H_2O, the activation barrier is lowered significantly (TPSSh, 0.96 eV; B3LYP, 1.17 eV). Again, the O_2 splitting on Au_6^- might be even lower because of some contribution from the favorable O_2 binding, suggesting that this reaction is viable at ambient conditions.

dx.doi.org/10.1021/cs300383p | ACS Catal. 2012, 2, 2614−2621

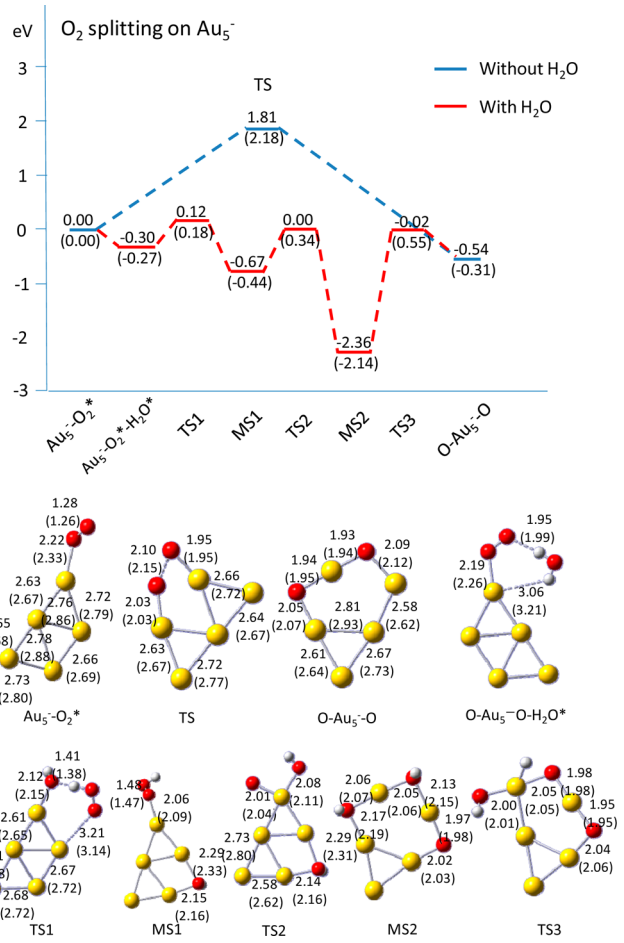

Figure 6. Calculated reaction pathway from the $Au_5^-(O_2)$ complex to dissociative O−Au_5^-−O using the TPSSh functional (B3LYP results in parentheses). The unit of bond length is the angstrom; an asterisk indicates attached.

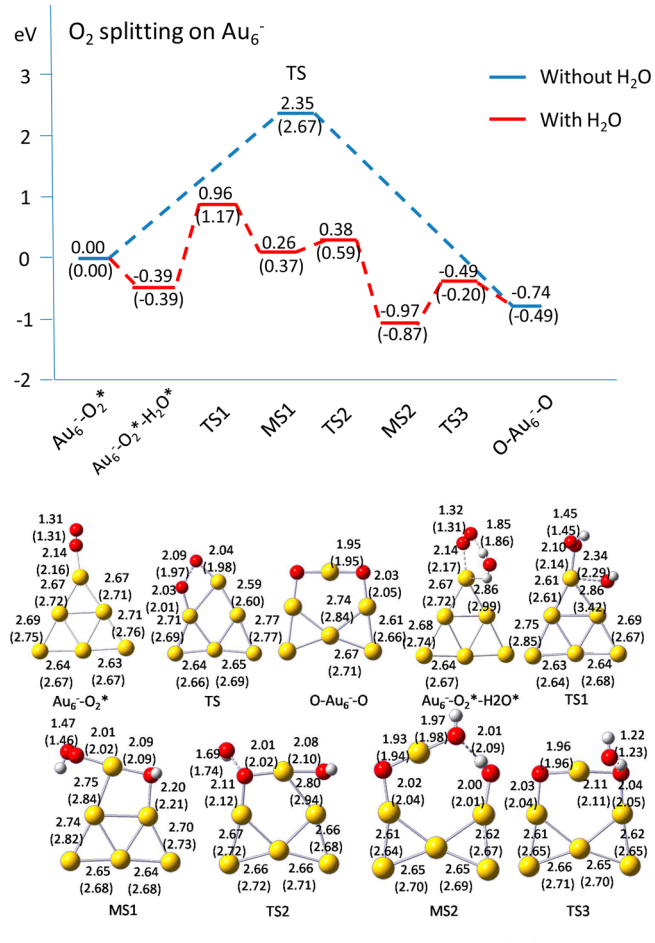

Figure 7. Calculated reaction pathway from the $Au_6^-(O_2)$ complex to dissociative O−Au_6^-−O using the TPSSh level of theory (B3LYP results in parentheses). The unit of bond length is the angstrom; an asterisk indicates the binding state.

Chemistry Behind O_2 Splitting with H_2O. The bond energy of O−O and O═O is 1.52 and 5.16 eV,[62] respectively. Hence, direct splitting of the O═O double bond would require considerably more energy than the splitting of the O−O bond. When H_2O is introduced in the O_2 splitting reaction, H could easily migrate from H_2O to O_2 with the assistance of gold clusters to transform the O═O double bond to an O−O single bond. As a result, the subsequent step to split a O−O single bond would be much easier than to split an O═O double bond. This process has been shown above.

Furthermore, if one considers introduction of reductant (e.g., CO) into the reaction, the reductant CO would react with either the atomic O or the hydroxyl group to form CO_2 and H_2O directly. Figure 8 displays an example in which CO is introduced into the O_2-splitting reaction on Au_4^-. As shown in Figure 5, MS2 is the most stable intermediate with one atomic O and 2 OH attaching to the Au_4^- cluster. When a CO attacks the atomic O atom, it yields a CO_2 molecule with a low activation barrier (TPSSh, 0.16 eV; B3LYP, 0.24 eV). Next, the second CO attacks an OH group to form a carboxyl group (**MS2**−**MS3**), for which the activation energy barrier is also low (TPSSh, 0.22 eV; B3LYP, 0.43 eV). The carboxyl group can react with the remaining OH group to release another CO_2 and one H_2O. The activation energy barrier (TPSSh, 0.17 eV; B3LYP, 0.14 eV) of this step is very low, as well. An alternative competing reaction pathway is that the carboxyl group may

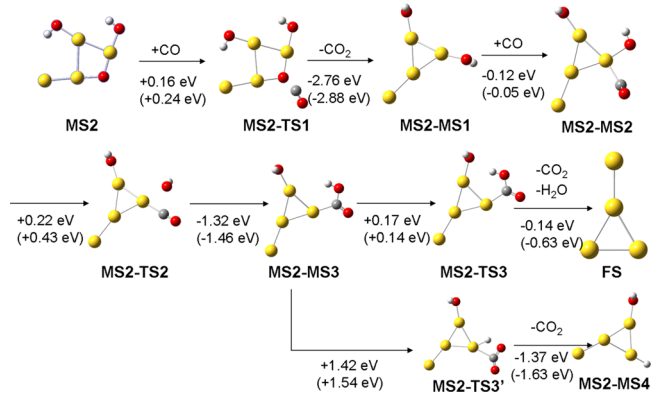

Figure 8. Calculated reaction pathways with a CO introduced in the MS2 stage (see Figure 5) and the MS2−MS1 stage for the O_2 splitting with H_2O on Au_4^-, using the TPSSh level of theory (B3LYP results in parentheses).

split into H and CO_2, but the associated activation energy barrier is very high (TPSSh, 1.42 eV; B3LYP, 1.54 eV) and, thus, is unlikely to occur.

It should be noted that two possible roles for H_2O in CO oxidation have been proposed in previous experimental studies: (1) activation of oxygen and (2) decomposition of carbonate.[40,63] Here, our calculations support the notion of

dx.doi.org/10.1021/cs300383p | ACS Catal. 2012, 2, 2614−2621

activation of oxygen.[63] Our calculation also suggests that the OH group in the reaction intermediate can react with the carbonate group directly to form CO_2 and H_2O, consistent with a previous experimental study.[64]

CONCLUSION

We present a systematic theoretical study of O_2 dissociation on small-sized anionic gold clusters (Au_n^-, n = 1−6). In most cases, the dissociative dioxide species are more stable than the O_2 molecular adsorption species on small-sized gold anionic clusters Au_n^- (except n = 2). However, the more stable dissociative dioxide species cannot be realized at room temperature because of the very high activation barrier (>2.0 eV) for the O_2 splitting. In practice, a more viable way to achieve O_2 dissociation on small-sized anionic Au clusters is to involve water as a promoter. With the involvement of a H_2O molecule, the O_2 dissociation barriers are significantly lowered. The activation barrier is reduced to 1.0 eV or lower, indicating that the reactions can proceed at room temperature. Once O_2 is dissociated, atomic oxygen is readily available for other reactions, such as the CO oxidation, on the surface of gold nanoclusters. This study thus points out an alternative way to exploit the catalytic capability of gold clusters for oxidation applications.

ASSOCIATED CONTENT

Supporting Information

Complete reference 56, O_2 binding energies with large basis sets, the complete reaction pathways with singlet and triplet states for Au^-, Au_3^- and Au_5^-. This material is available free of charge via the Internet at http://pubs.acs.org.

AUTHOR INFORMATION

Corresponding Author

*E-mail: gaoyi@sinap.ac.cn; xzeng1@unl.edu.

Notes

The authors declare no competing financial interest.

ACKNOWLEDGMENTS

Y.G. is supported by the startup funding from Shanghai Institute of Applied Physics, Chinese Academy of Sciences (Y290011011), and National Natural Science Foundation of China (21273268). X.C.Z. is supported by grants from the NSF (EPS-1010674) and ARL (W911NF1020099) and by the University of Nebraska's Holland Computing Center. Y.G. is grateful for the support from the Supercomputing Center of Chinese Academy of Sciences in Beijing, Shanghai Supercomputer Center, and National Supercomputing Center Shenzhen.

REFERENCES

(1) Haruta, M.; Kobayashi, T.; Samo, H.; Yamada, N. *Chem. Lett.* **1987**, 405−408.
(2) Haruta, M.; Yamada, N.; Kobayashi, T.; Ijima, S. *J. Catal.* **1989**, *115*, 301−309.
(3) Lizuka, Y.; Fujiki, H.; Yamauchi, N.; Chijiiwa, T.; Arai, S.; Tsubota, S.; Haruta, M. *Catal. Today* **1997**, *36*, 115−123.
(4) Haruta, M. *Catal. Today* **1997**, *36*, 153−166.
(5) Bond, G. C. *Catal. Today* **2002**, *72*, 5−9.
(6) Wesendrup, R.; Hunt, T.; Schwerdtfeger, P. *J. Chem. Phys.* **2000**, *112*, 9356−9362.
(7) Häkkinrn, H.; Landman, U. *Phys. Rev. B* **2000**, *62*, R2287.
(8) Häkkinrn, H.; Moseler, M.; Landman, U. *Phys. Rev. Lett.* **2002**, *89*, 033401.
(9) Pyykkö, P. *Relativistic Theory of Atoms and Molecules*; Springer: Berlin, 2000; Vol. *III*, pp 108−111.
(10) Pyykkö, P. *Angew. Chem., Int. Ed.* **2004**, *43*, 4412−4456.
(11) Pyykkö, P. *Chem. Soc. Rev.* **2008**, *37*, 1967−1997 and references therein..
(12) Schwarz, H. *Angew. Chem., Int. Ed.* **2003**, *42*, 4442−4454.
(13) Gao, Y.; Shao, N.; Bulusu, S.; Zeng, X. C. *J. Phys. Chem. C* **2008**, *112*, 8234−8238.
(14) Gao, Y.; Shao, N.; Pei, Y.; Zeng, X. C. *Nano Lett.* **2010**, *10*, 1055−1062.
(15) Gao, Y.; Shao, N.; Pei, Y.; Chen, Z.; Zeng, X. C. *ACS Nano* **2011**, *5*, 7818−7829.
(16) Patil, N. S.; Uphade, B. S.; Jana, P.; Sonawane, R. S.; Bhargava, S. K.; Choudhary, V. R. *Catal. Lett.* **2004**, *94*, 89−93.
(17) Patil, N. S.; Uphade, B. S.; Jana, P.; Bharagava, S. K.; Choudhary, V. R. *J. Catal.* **2004**, *223*, 236−239.
(18) Patil, N. S.; Uphade, B. S.; Jana, P.; Bhargava, S. K.; Choudhary, V. R. *Chem. Lett.* **2004**, *33*, 400−401.
(19) Patil, N. S.; Uphade, B. S.; Jana, P.; Bhargava, S. K.; Choudhary, V. R. *Appl. Catal., A* **2004**, *275*, 87−93.
(20) Deng, X.; Friend, C. M. *J. Am. Chem. Soc.* **2005**, *127*, 17178−17179.
(21) Cox, D. M.; Brickman, R.; Creegan, K.; Kaldor, A. *Z. Phys. D* **1991**, *19*, 353−355.
(22) Cox, D. M.; Brickman, R. O.; Creegan, K.; Kaldor, A. *Kinetics Saturation Mater. Res. Soc. Symp. Proc.* **1991**, *206*, 34−39.
(23) Lee, T. H.; Ervin, K. M. *J. Phys. Chem.* **1994**, *98*, 10023−10031.
(24) Salisbury, B. E.; Wallace, W. T.; Whetten, R. L. *Chem. Phys.* **2000**, *262*, 131−141.
(25) Wallace, W. T.; Leavitt, A. J.; Whetten, R. L. *Chem. Phys. Lett.* **2003**, *368*, 774−777.
(26) Huang, W.; Zhai, H.-J.; Wang, L. S. *J. Am. Chem. Soc.* **2010**, *132*, 4344−4351.
(27) Pal, R.; Wang, L.-M.; Pei, Y.; Wang, L. S.; Zeng, X. C. *J. Am. Chem. Soc.* **2012**, *134*, 9438−9445.
(28) Woodham, A. P.; Meijer, G.; Fielicke, A. *Angew. Chem., Int. Ed.* **2012**, *51*, 4444−4447.
(29) Mills, G.; Gordon, M. S.; Metiu, H. *Chem. Phys. Lett.* **2002**, *359*, 493.
(30) Ding, X.; Li, Z.; Yang, J.; Hou, J. G.; Zhu, Q. *J. Chem. Phys.* **2004**, *120*, 9594−9600.
(31) Molina, L. M.; Hammer, B. *J. Chem. Phys.* **2005**, *123*, 161104.
(32) Barton, D. G.; Podkolzin, S. G. *J. Phys. Chem. B* **2005**, *109*, 2262−2274.
(33) Yoon, B.; Hakkinen, H.; Landman, U. *J. Phys. Chem. A* **2003**, *107*, 4066−4071.
(34) Wang, Y.; Gong, X. G. *J. Chem. Phys.* **2006**, *125*, 124703.
(35) Barrio, L.; Liu, P.; Rodriguez, J. A.; Campos-Martin, J. M.; Fierro, J. L. G. *J. Phys. Chem. C* **2007**, *111*, 19001−19008.
(36) Lyalin, A.; Taketsugu, T. *J. Phys. Chem. Lett.* **2010**, *1*, 1752−1757.
(37) Zhai, H.-J.; Bürgel, C.; Bonacic-Koutecky, V.; Wang, L.-S. *J. Am. Chem. Soc.* **2008**, *130*, 9156−9167.
(38) Gao, Y.; Huang, W.; Woodford, J.; Wang, L. S.; Zeng, X. C. *J. Am. Chem. Soc.* **2009**, *131*, 9484−9485.
(39) Boccuzzi, F.; Chiorino, A. *J. Phys. Chem. B* **2000**, *104*, 5414−5416.
(40) Daté, M.; Okumura, M.; Tsubota, S.; Haruta, M. *Angew. Chem., Int. Ed.* **2004**, *43*, 2129−2132.
(41) Bond, G. C.; Thompson, D. T. *Gold. Bull.* **2000**, *33*, 41−50.
(42) Bongiorno, A.; Landman, U. *Phys. Rev. Lett.* **2005**, *95*, 106102.
(43) Kim, T. S.; Gond, J.; Ojifinni, R. A.; White, J. M.; Mullins, C. B. *J. Am. Chem. Soc.* **2006**, *128*, 6282−6283.
(44) Wallace, W. T.; Wyrwas, R. B.; Whetten, R. L.; Mitrić, R.; Bonačić Koutecký, V. *J. Am. Chem. Soc.* **2003**, *125*, 8408−8414.
(45) Okumura, M.; Haruta, M.; Kitagawa, Y.; Yamaguchi, K. *Gold Bull.* **2007**, *40*, 40−44.

(46) Zhang, W. H.; Li, Z. Y.; Luo, Y.; Yang, J. L. *Chin. Sci. Bull.* **2009**, *54*, 1973−1977.
(47) Lee, S.; Monlina, L. M.; López, M.; Alonso, J. A.; Hammer, B.; Lee, B.; Seifert, S.; Winans, R. E.; Elam, J. W.; Pellin, M. J.; Vajda, S. *Angew. Chem., Int. Ed.* **2009**, *48*, 1467−1471.
(48) Becke, A. D. *Phys. Rev. A* **1988**, *38*, 3098.
(49) Lee, C.; Yang, W.; Parr, R. G. *Phys. Rev. B* **1988**, *37*, 785−789.
(50) Tao, J. M.; Perdew, J. P.; Staroverov, V. N.; Scuseria, G. E. *Phys. Rev. Lett.* **2011**, *91*, 146401.
(51) Shi, Y.-K.; Li, Z. H.; Fan, K.-N. *J. Phys. Chem. A* **2010**, *114*, 10297−10308.
(52) Dolg, M.; Wedig, U.; Stoll, H.; Preuss, H. *J. Chem. Phys.* **1987**, *86*, 866.
(53) Schwerdtfeger, P.; Dolg, M.; Schwarz, W. H. E.; Bowmaker, G. A.; Boyd, P. D. W. *J. Chem. Phys.* **1989**, *91*, 1762.
(54) Peng, C.; Schlegel, H. B. *Isr. J. Chem.* **1993**, *33*, 449−454.
(55) Peng, C.; Ayala, P. Y.; Schlegel, H. B.; Frisch, M. J. *J. Comput. Chem.* **1996**, *17*, 49−56.
(56) Frisch, M. J., et al. *Gaussian09, Revision A.02*; Gaussian, Inc., Wallingford CT, 2009.
(57) Häkkinen, H.; Yoon, B.; Landman, U.; Li, X.; Zhai, H.-J.; Wang, L. S. *J. Phys. Chem. A* **2003**, *107*, 6168−6175.
(58) Zhang, C.; Michaelides, A.; King, D. A.; Jenkins, S. J. *J. Am. Chem. Soc.* **2010**, *132*, 2175−2182.
(59) Glendening, E. D.; Reed, A. E.; Carpenter, J. E.; Weinhold, F. *NBO version 3.1*, 1995.
(60) Smith, T. *J. Colloid Interface Sci.* **1980**, *75*, 51−55.
(61) Röckmann, T.; Brenninkmeijer, C. A. M.; Saueressig, G.; Bergamaschi, P.; Crowley, J. N.; Fischer, H.; Crutzen, P. J. *Science* **1998**, *281*, 544−546.
(62) The standard bond energy data is coming from the website of http://www.cem.msu.edu/~reusch/OrgPage/bndenrgy.htm.
(63) Boccuzzi, F.; Chiorino, A.; Manzoli, M.; Lu, P.; Akita, T.; Ichikawa, S.; Haruta, M. *J. Catal.* **2001**, *202*, 256−267.
(64) Costello, C. K.; Yang, J. H.; Law, H. Y.; Wang, Y.; Lin, J.-N.; Marks, L. D.; Kung, M. C.; Kung, H. H. *Appl. Catal., A* **2003**, *243*, 15−24.